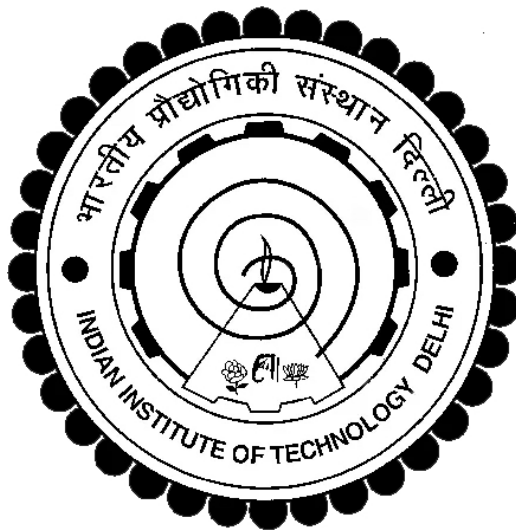


**FROM NUCLEATION TO HAZE: AEROSOL  
EVOLUTION IN POLLUTED  
ENVIRONMENTS**

**UMER ALI**



**DEPARTMENT OF CHEMICAL ENGINEERING  
INDIAN INSTITUTE OF TECHNOLOGY DELHI**

**JULY 2025**

© Indian Institute of Technology Delhi (IITD), New Delhi, 2025

ALL RIGHTS RESERVE

# **FROM NUCLEATION TO HAZE: AEROSOL EVOLUTION IN POLLUTED ENVIRONMENTS**

**By**

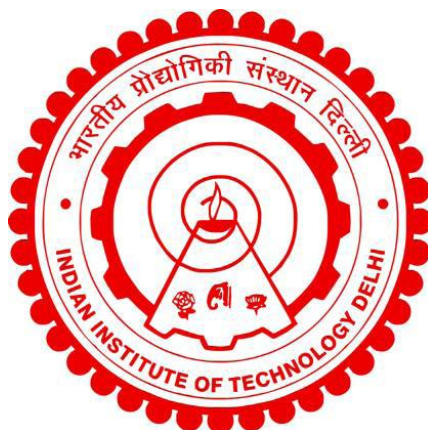
**Umer Ali**

Department of Chemical Engineering

*Submitted*

in fulfilment of the requirements of the degree of Doctor of Philosophy

to the



**INDIAN INSTITUTE OF TECHNOLOGY DELHI**

**JULY 2025**

***"And do not cause corruption upon the earth after its reformation."***

***(Qur'an 7:56)***

*With deep gratitude and reverence, I dedicate this work:*

*To Allah, the Most Gracious, the Wisest, the Giver of knowledge and the Sustainer of all that exists.*

*To all His noble Messengers, who illuminated the world with guidance, truth, and compassion.*

*And to the priceless gift of clean air, an unseen blessing that sustains life and reminds us of our sacred duty to protect and cherish the Earth.*

## **Certificate**

This is to certify that the thesis entitled “From Nucleation to Haze: Aerosol Evolution in Polluted Environments”, submitted by Umer Ali to the Indian Institute of Technology Delhi, for the award of the degree of Doctor of Philosophy in Chemical Engineering, is a record of the original, Bonafide research work carried out by him under our supervision and guidance. The thesis has reached the standards fulfilling the requirements of the regulations related to the award of the degree.

The results contained in this thesis have not been submitted in part or in full to any other University or Institute for the award of any degree or diploma to the best of our knowledge.

**Prof. Vikram Singh**

Department of Chemical Engineering,  
Indian Institute of Technology Delhi.

**Prof. Mayank Kumar**

Department of Mechanical Engineering,  
Indian Institute of Technology Delhi

New Delhi  
June 2025

## Acknowledgements

The redemption of all joy and reward is founded on a simple yet profound emotion – gratitude. While it is never possible to fully repay the acts of kindness and goodness bestowed upon me, these humble words aim to express the awe and admiration I feel as I reach a pivotal milestone in my career: the completion of my doctoral education.

When I embarked on this PhD journey, I had a little understanding of the path that lay ahead. I am deeply thankful to Allah for granting me the opportunity to seek knowledge, for surrounding me with supportive mentors, colleagues, friends, and family, and for guiding me to the successful completion of this chapter in my life. Indeed, all success and accomplishments are solely by His will. Alhamdulillah!

I am profoundly grateful to my supervisors, Prof. Vikram Singh and Prof. Mayank Kumar, for their unwavering commitment to clarity, depth of understanding, and pursuit of excellence. Their mentorship has not only refined my research but also instilled in me the value of precision and critical thinking. Their constant encouragement and constructive feedback have been instrumental in shaping both my academic and personal growth. I feel incredibly fortunate to have had supervisors who are not only exceptional mentors but also genuinely kind and inspiring individuals. Prof. Vikram Singh has always offered the affection and warmth essential for an early-stage researcher, and I extend my sincere gratitude to him. I am deeply grateful to Prof. Shahzad Gani for his invaluable guidance and unwavering support throughout this research journey. His timely advice and mentorship have been instrumental in shaping this work.

I extend my sincere appreciation to the esteemed members of my Research Assessment Panel at the Indian Institute of Technology Delhi—Prof. Shantanu Roy, Prof. Divesh Bhatia, and Prof. Dilip Ganguly—for their insightful suggestions during progress review meetings, which significantly enhanced the quality of this research. My heartfelt thanks to the Department of Chemical Engineering, IIT Delhi, for providing an excellent academic environment, state-of-the-art infrastructure, and the necessary resources to conduct this study. I also acknowledge with gratitude the financial support received from the IRD Grand Challenge Project Grant (Grant No. 428 IITD/IRD/MI01810G), funded by the Ministry of Education (formerly MHRD), Government of India, which made this research possible.

To my wonderful family, who have stood by me through every decision, I am eternally grateful. My beloved parents, whose unconditional love, prayers, and sacrifices have been the cornerstone of my journey, deserve my deepest appreciation. Their unwavering support, encouragement, and belief in my abilities have been my greatest source of strength. From their countless prayers for my success to the sacrifices they made to ensure I could pursue my dreams; I owe everything to their love and dedication. Their guidance, wisdom, and values have shaped the person I am today, and this achievement is as much theirs as it is mine. To my dearest grandparents, your blessings, values, and prayers have always guided me. To my loving sisters, thank you for your constant encouragement, affection, and belief in me. Your presence has always been a source of comfort and motivation. And to a very special person, Saima, your love, patience, and unwavering support throughout this journey have meant the world to me. I eagerly look forward to the life ahead with you by my side. To all my extended family members, your love, prayers, and well wishes have played a vital role in this journey. I am truly blessed to have such a strong and supportive family around me.

I have been blessed with wonderful colleagues and friends who have made this journey memorable. Dr. Faisal, Ajit, Dr. Asad, Dr Naba Hazarika, Sombir, Anjanay, Sayan, and Aamir have been pillars of support and respect throughout the PhD. Their friendship has been a source of strength and camaraderie, and I am deeply grateful to them. The PhD journey has also introduced me to incredible individuals who have become lifelong friends. Faiz and Saqib, sharing a flat with you for the last 3 and half years was an adventure, and the fact that we are still talking is a testament to our enduring friendship. The countless memories – the ups and downs, laughter, and shared experiences – are treasures I will always cherish. Aadil Bashir, Rafiq, Mujeeb, Danish, Adnan, Sarfraz, Saleem, and Mustansir, I express my deepest gratitude for your exemplary love, friendship, support, and respect. Although it's impossible to name everyone individually, I am profoundly thankful to all my friends at the Indian Institute of Technology Delhi for their comforting kinship and unwavering support. Your presence has been a vital part of this journey. To my childhood friends Aadil Bilal, Ishfaq, Aamir Fayaz, Aamir Hassan, Waseem, and Wajahat, thank you for your enduring love, emotional support, and belief in me throughout the years.

This journey has been a collective effort, and I am forever indebted to everyone who has contributed to its success. Thank you.

## Abstract

Fine particulate matter (PM<sub>2.5</sub>) adversely impacts human health, climate, air quality, and visibility, necessitating effective mitigation strategies. Addressing these challenges requires a thorough understanding chemical composition, physical properties (e.g., hygroscopicity, phase state), and atmospheric interactions (e.g., gas-particle partitioning, secondary formation) of PM<sub>2.5</sub>. However, persistent knowledge gaps, particularly in quantifying sources, formation pathways, and thermodynamic behaviour, hinder region-specific policy development, especially in pollution hotspots like the Indo-Gangetic Plain (IGP). This study investigates two critical aerosol processes in Delhi, a representative IGP megacity: (1) new particle formation (NPF) and (2) hygroscopic water uptake driving aerosol liquid water content (ALWC). Using real-time non-refractory PM<sub>2.5</sub> (NR-PM<sub>2.5</sub>) data from an Aerodyne Aerosol Chemical Speciation Monitor (ACSM) and thermodynamic modelling (ISORROPIA II), we analysed ALWC dynamics for two winter periods (Dec 2019–Jan 2020 and Dec 2020–Feb 2021). A 50% increase in average NR-PM<sub>2.5</sub> concentrations (from 102  $\mu\text{g}/\text{m}^3$  to 152  $\mu\text{g}/\text{m}^3$ ) resulted in a 60% rise in ALWC, which exhibited exponential growth with relative humidity (RH), becoming significant at RH >80%. Ammonium sulphate dominated ALWC uptake at lower RH, while ammonium nitrate prevailed at higher RH. Elevated PM<sub>2.5</sub> and RH significantly reduced visibility, with light scattering efficiency increasing by more than 3.5 times at RH >85%. Chloride (Cl) concentrations in PM<sub>2.5</sub> have halved in recent years, reducing their contribution to ALWC. While nitrate and sulphate, the other major contributors to ALWC, are linked to power plants and vehicular emissions, the sources of chloride remain poorly understood. Source apportionment studies in Delhi have struggled to identify the exact sources of chloride due to weak correlations with primary tracers. This study investigated one potential source of chloride: crop residue (stubble) burning. Real-time PM<sub>2.5</sub> chemical composition data from stubble burning hotspots in rural Punjab during peak stubble burning demonstrated strong correlations between Cl and primary biomass burning tracers (potassium; K, organic aerosols; OA, black carbon; BC). Elemental source apportionment in Punjab attributed ~80% of chloride to stubble burning, supported by diagnostic Cl/K molar ratios (~2), indicative of gaseous chloride emissions beyond potassium chloride (KCl). In contrast, Delhi's chloride dynamics were predominantly governed by meteorological processes, with secondary chloride formation contributing 70–80% of total chloride and biomass burning accounting for only 10–20%. Diagnostic ratios (Cl/K, Cl/OA, Cl/BC) in Delhi revealed a complex mix of sources: post-monsoon chloride signatures aligned with Punjab's stubble burning, while elevated Cl/K ratios

in other seasons (summer, winter) pointed to non-biomass sources like waste burning or industrial emissions. We also investigated the seasonal characteristics of particle size distribution (PSD) in Delhi's atmosphere, with a special focus on NPF. Our findings reveal pronounced seasonal variations in particle number and mass concentration levels following the variations in atmospheric conditions and emission sources across different seasons. Condensation sink (CS) emerged as a primary factor governing NPF, with no NPF events observed when daytime CS exceeded  $0.06 \text{ s}^{-1}$ . NPF events were characterized by relatively high formation rates, high sulphuric acid concentrations, and a relatively large CS compared to cleaner and more pristine environments. The estimated formation rates were comparable to other polluted regions and could be explained by mechanisms involving  $\text{H}_2\text{SO}_4$ , ammonia and amines like dimethylamine (DMA). On days with comparable CS, chemical composition showed no significant variation between NPF and non-NPF days, with organics contributing  $\sim 50\%$  of  $\text{PM}_{2.5}$ , emphasizing the dominance of physical processes. Higher atmospheric liquid water content, driven by elevated RH, inhibited NPF, highlighting the critical influence of relative humidity on particle formation. Additionally, simultaneous analysis of PSD and  $\text{PM}_{2.5}$  mass composition revealed significant variations during daytime and night-time growth phases. Daytime growth of nucleated particles was associated with increases in sulphate and low-volatility oxygenated organics, suggesting the involvement of sulphuric acid and oxidized vapours in early particle growth. This study highlights the need for comprehensive, long-term monitoring of ALWC, PSD, and  $\text{PM}_{2.5}$  chemical composition to address Delhi's air quality challenges. Mitigation strategies should prioritize reducing inorganic  $\text{PM}_{2.5}$  concentrations to lower ALWC and improve visibility, while at the same time focus on controlling precursor gases such as sulphuric acid and organic vapours to limit the formation of ultrafine particles, which have significant health and climate impacts.

## सारांश

सूक्ष्म कणिकीय पदार्थ (PM<sub>2.5</sub>) मानव स्वास्थ्य, जलवायु, वायु गुणवत्ता और दृश्यता पर प्रतिकूल प्रभाव डालता है, जिससे प्रभावी न्यूनीकरण रणनीतियों की आवश्यकता होती है। इन चुनौतियों का समाधान करने के लिए PM<sub>2.5</sub> के रासायनिक संघटन, भौतिक गुणों (जैसे, जल-अवशोषण क्षमता, अवस्था) और वायुमंडलीय अंतःक्रियाओं (जैसे, गैस-कण विभाजन, द्वितीयक निर्माण) की गहन समझ आवश्यक है। हालांकि, विशेष रूप से स्रोतों, निर्माण मार्गों और ऊष्मागतिक व्यवहार के मात्रात्मक आकलन में ज्ञान की कमी, क्षेत्र-विशेष नीति निर्माण में बाधा उत्पन्न करती है, खासकर इंडो-गंगेटिक प्लेन (IGP) जैसे प्रदूषण हॉटस्पॉट में। यह अध्ययन दिल्ली, एक प्रतिनिधि IGP महानगर, में दो महत्वपूर्ण एरोसोल प्रक्रियाओं की जांच करता है: (1) नए कण निर्माण (NPF) और (2) जल-अवशोषण द्वारा एरोसोल द्रव जल सामग्री (ALWC) का निर्माण। एरोडाइन एरोसोल केमिकल स्पेशिएशन मॉनिटर (ACSM) से प्राप्त वास्तविक समय के गैर-दहनशील PM<sub>2.5</sub> (NR-PM<sub>2.5</sub>) डेटा और ऊष्मागतिक मॉडलिंग (ISORROPIA II) का उपयोग करते हुए, हमने दो शीतकालीन अवधियों (दिसंबर 2019–जनवरी 2020 और दिसंबर 2020–फरवरी 2021) के लिए ALWC की गतिशीलता का विश्लेषण किया। NR-PM<sub>2.5</sub> की औसत सांद्रता में 50% की वृद्धि (102  $\mu\text{g}/\text{m}^3$  से 152  $\mu\text{g}/\text{m}^3$ ) के परिणामस्वरूप ALWC में 60% की वृद्धि हुई, जो सापेक्ष आर्द्रता (RH) के साथ घातीय रूप से बढ़ी और RH >80% पर महत्वपूर्ण हो गई। अमोनियम सल्फेट ने कम RH पर ALWC अवशोषण पर प्रभुत्व दिखाया, जबकि अमोनियम नाइट्रेट उच्च RH पर प्रभावी था। उच्च PM<sub>2.5</sub> और RH ने दृश्यता को काफी कम कर दिया, जहाँ RH >85% पर प्रकाश प्रकीर्णन दक्षता 3.5 गुना से अधिक बढ़ गई। हाल के वर्षों में PM<sub>2.5</sub> में क्लोराइड (Cl) सांद्रता आधी हो गई है, जिससे ALWC में उनका योगदान कम हुआ है। हालांकि, नाइट्रेट और सल्फेट, जो ALWC के अन्य प्रमुख योगदानकर्ता हैं, बिजली संयंत्रों और वाहन उत्सर्जन से जुड़े हैं, क्लोराइड के स्रोत अभी भी अस्पष्ट हैं। दिल्ली में स्रोत विभाजन अध्ययनों में क्लोराइड के सटीक स्रोतों की पहचान करने में कठिनाई हुई है क्योंकि यह प्राथमिक ट्रेसर्स के साथ कमजोर सहसंबंध दिखाता है। इस अध्ययन में क्लोराइड के एक संभावित स्रोत-फसल अवशेष (पराली) जलाने-की जाँच की गई। पंजाब के ग्रामीण क्षेत्रों में पराली जलाने के चरम समय के दौरान वास्तविक समय PM<sub>2.5</sub> रासायनिक संघटन डेटा ने Cl और प्राथमिक बायोमास जलने के ट्रेसर्स (K, OA, BC) के बीच मजबूत सहसंबंध दिखाया। पंजाब में तत्व-आधारित स्रोत विभाजन ने ~80% क्लोराइड को पराली जलाने से जोड़ा, जिसे Cl/K मोलर अनुपात (~2) द्वारा समर्थित किया गया, जो KCl से परे गैसीय क्लोराइड उत्सर्जन का संकेत देता है। इसके विपरीत, दिल्ली में क्लोराइड गतिशीलता मुख्यतः मौसम संबंधी प्रक्रियाओं द्वारा नियंत्रित थी, जहाँ द्वितीयक क्लोराइड निर्माण कुल

क्लोराइड का 70–80% योगदान देता है और बायोमास जलाने का योगदान केवल 10–20% है। दिल्ली में नैदानिक अनुपात (C1/K, C1/OA, C1/BC) ने स्रोतों का एक जटिल मिश्रण दिखाया: मानसून के बाद के क्लोराइड संकेत पंजाब के पराली जलाने से मेल खाते थे, जबकि अन्य मौसमों (गर्मी, सर्दी) में उच्च C1/K अनुपात ने गैर-बायोमास स्रोतों (जैसे कचरा जलाना या औद्योगिक उत्सर्जन) की ओर इशारा किया। हमने दिल्ली के वायुमंडल में कण आकार वितरण (PSD) की मौसमी विशेषताओं का भी अध्ययन किया, विशेष रूप से NPF पर ध्यान केंद्रित करते हुए। हमारे निष्कर्षों से पता चलता है कि वायुमंडलीय परिस्थितियों और उत्सर्जन स्रोतों में मौसमी परिवर्तनों के अनुसार कण संख्या और द्रव्यमान सांद्रता में स्पष्ट मौसमी भिन्नताएँ होती हैं। संघनन सिंक (CS) NPF को नियंत्रित करने वाला प्राथमिक कारक था, जहाँ दिन के समय  $CS > 0.06 \text{ s}^{-1}$  होने पर कोई NPF घटना नहीं देखी गई। NPF घटनाओं की विशेषता उच्च निर्माण दर, उच्च सल्फ्यूरिक अम्ल सांद्रता और उच्च CS थी। अनुमानित निर्माण दरें अन्य प्रदूषित क्षेत्रों के समान थीं और H<sub>2</sub>SO<sub>4</sub> तथा एमाइन्स (डाइमिथाइलएमाइन (DMA) और अमोनिया सहित) से जुड़े तंत्रों द्वारा समझाई जा सकती हैं। CS की तुलनीय स्थितियों वाले दिनों में, NPF और गैर-NPF दिनों के बीच रासायनिक संघटन में कोई महत्वपूर्ण अंतर नहीं था, जहाँ कार्बनिक पदार्थ PM<sub>2.5</sub> का ~50% योगदान देते थे, जो भौतिक प्रक्रियाओं के प्रभुत्व को दर्शाता है। उच्च RH के कारण वायुमंडलीय द्रव जल सामग्री में वृद्धि ने NPF को रोका, जो कण निर्माण पर सापेक्ष आर्द्रता के महत्वपूर्ण प्रभाव को उजागर करता है। इसके अतिरिक्त, PSD और PM<sub>2.5</sub> द्रव्यमान संघटन का एक साथ विश्लेषण करने से दिन और रात के विकास चरणों के दौरान महत्वपूर्ण भिन्नताएँ देखी गईं। न्यूक्लियेटेड कणों का दिन के समय विकास सल्फेट और कम-वाष्पशील ऑक्सीजनयुक्त कार्बनिक पदार्थों में वृद्धि से जुड़ा था, जो सल्फ्यूरिक अम्ल और ऑक्सीकृत वाष्पों की भूमिका को प्रारंभिक कण विकास में दर्शाता है। यह अध्ययन दिल्ली की वायु गुणवत्ता चुनौतियों का समाधान करने के लिए ALWC, PSD और PM<sub>2.5</sub> रासायनिक संघटन की व्यापक, दीर्घकालिक निगरानी की आवश्यकता को रेखांकित करता है। न्यूनीकरण रणनीतियों को अकार्बनिक PM<sub>2.5</sub> सांद्रता को कम करके ALWC को कम करने और दृश्यता में सुधार करने पर ध्यान केंद्रित करना चाहिए, साथ ही सल्फ्यूरिक अम्ल और कार्बनिक वाष्पों जैसे पूर्वगामी गैसों को नियंत्रित करना चाहिए ताकि अति सूक्ष्म कणों के निर्माण को सीमित किया जा सके, जिनका स्वास्थ्य और जलवायु पर महत्वपूर्ण प्रभाव पड़ता है।

## Table of Contents

Certificate.....	v
Acknowledgements.....	ii
Abstract.....	iv
Table of Contents .....	viii
List of Figures.....	xiii
List of Tables.....	xix
Chapter 1: Introduction.....	20
1.1 Motivation.....	20
1.2 Research Objectives and Aims.....	23
1.3 Thesis Outline: .....	24
References.....	27
Chapter 2: Literature Review .....	35
2.1 Background: Atmospheric aerosols and Particulate Matter (PM) .....	35
2.2 PM <sub>2.5</sub> characteristics- size, sources, and formation pathways.....	36
2.3 PM constituents and ALWC.....	39
2.3.1 ALWC uptake mechanism .....	40
2.3.2 Measurement of ALWC .....	43
2.3.3 Indo-Gangetic Plains and Delhi.....	44
2.4 Contribution of chloride to ALWC and sources of chloride .....	48
2.5 New Particle Formation (NPF) .....	51
2.5.1 NPF mechanisms and governing factors.....	53
2.5.2 NPF in Delhi and IGP .....	56
References.....	58
Chapter 3: Methodology .....	78
3.1 Sampling site:.....	78
3.2 Instrumentation and Data acquisition: .....	79
3.2.1 Non-refractory PM <sub>2.5</sub> (NR-PM <sub>2.5</sub> ) .....	79
3.2.2 Elemental PM <sub>2.5</sub> Composition: .....	79

3.2.3 Black Carbon (BC): .....	80
3.2.4 Submicron Particle Size Distribution: .....	80
3.2.5 Sampling description .....	80
3.3 Trace Gases and Meteorological Parameters .....	81
References.....	83
Chapter 4: Analysis of aerosol liquid water content and its role in visibility reduction in Delhi .....	85
4.1 Introduction.....	87
4.2 Materials and Methodology .....	89
4.2.1 Sampling Site and Instrumentation.....	89
4.2.2 Aerosol Liquid Water Content .....	90
4.2.3 Chemical composition-based hygroscopicity parameter .....	91
4.2.4 $f(\text{RH})$ derived from visibility and $\text{PM}_{2.5}$ .....	92
4.2.5 $f(\text{RH})$ derived from the hygroscopicity parameter.....	92
4.3 Results and Discussion .....	93
4.3.1 Mass Concentration of different $\text{PM}_{2.5}$ components .....	93
4.3.2 The ALWC levels for two winter campaigns.....	96
4.3.3 Comparison of meteorological conditions for two winters.....	100
4.3.4 Contribution of $\text{PM}_{2.5}$ components to ALWC .....	103
4.3.5 Impact of ambient RH on ALWC .....	105
4.3.6 Effect of chemical composition on hygroscopicity.....	109
4.3.7 Role of ALWC in haze episodes .....	110
4.3.8 Effect of ALWC on visibility reduction.....	111
4.3.9 Reduction of Chloride mass concentration in recent years.....	113

4.4 Conclusion .....	115
Acknowledgment .....	117
References.....	118
Chapter 5: Exploring the influence of physical and chemical factors on new particle formation in a polluted megacity.....	125
Abstract.....	126
5.1 Introduction.....	127
5.2 Materials and methodology.....	129
5.2.1 Instrumentation and Data acquisition .....	129
5.2.2 Size-resolved particle concentrations .....	130
5.2.3 NPF Identification.....	131
5.2.4 Condensation Sink (CS).....	131
5.2.5 Growth Rate .....	132
5.2.6 Apparent ( $J_{10}$ ) and real nucleation ( $J_{1.5}$ ) rates .....	133
5.2.7 H <sub>2</sub> SO <sub>4</sub> Proxy .....	134
5.3 Results and Discussions.....	134
5.3.1 Aerosol PNC characterization.....	134
<i>Seasonal variation</i> .....	134
<i>Diel variations</i> .....	138
5.3.2 New particle formation .....	139
5.3.3 CS and New Particle Formation Events.....	141
5.3.4 Formation rates and mechanism .....	147
5.3.5 Role of meteorological parameters .....	150
5.3.6 Effect of Chemical Composition .....	151
5.3.7 New Particle Formation and Condensational Growth .....	154

5.4 Conclusion .....	160
Author contributions .....	161
Acknowledgments.....	161
References.....	162
Chapter 6: Investigation of the Contribution of Regional Crop Residue Burning to PM <sub>2.5</sub> -Bound Chloride in Delhi.....	178
6.1 Introduction.....	179
6.2 Materials and Methodology .....	181
6.2.1 Sampling sites .....	181
6.2.2 Instrumentation for PM <sub>2.5</sub> Mass Concentration and Characterization .....	183
6.2.3 Positive Matrix Factorization (PMF) Analysis .....	184
6.3 Results and Discussion .....	185
6.3.1 Seasonal and diel variations of chloride in Delhi .....	185
6.3.2 Possible Chloride sources and role of stubble burning.....	188
6.3.3 Close to Stubble Burning Hotspots in Punjab: Results and Observations.....	190
6.3.4 Source Apportionment Results .....	192
6.3.5 Temporal and Diel Variations of Stubble Burning Factor.....	193
6.3.6 Chloride from biomass burning and Implications in Delhi .....	195
6.3.7 Stubble-burning period (post-monsoon and Summer).....	196
6.3.8 Winter and Spring .....	198
6.4 Limitations .....	200
6.5 Conclusion .....	201
Acknowledgements.....	202
References.....	203
Chapter 7: Conclusion, limitations and future recommendations.....	211
<b>Limitations and Future Research Directions</b> .....	213
Appendix A .....	216

Appendix B .....	240
Appendix C .....	274
List of publications .....	287
Brief biodata.....	288

## List of Figures

- Figure 1.1: Schematic representation of particulate and trace gas emissions, their transformation and growth in the atmosphere, climate impacts, and potential health impacts. The sources of emissions include various anthropogenic and natural processes.....21
- Figure 2.1: Schematic representation of aerosol size distribution and transformation processes in the atmosphere. The diagram illustrates different aerosol modes—nucleation, Aitken, accumulation, and coarse—along with key processes such as condensation, coagulation, evaporation, and coalescence, which govern aerosol growth and removal. ....37
- Figure 2.2: Kelvin effect curves for water and dioctyl phthalate (DOP), showing the saturation ratio as a function of droplet diameter. The curves illustrate how smaller droplets require higher saturation ratios to remain in equilibrium due to surface curvature effects (Seinfeld & Pandis, 2016). ....42
- Figure 2.3: Hygroscopic growth hysteresis of aerosol particles, illustrating water uptake during humidification and water release during dehumidification. The distinct deliquescence and efflorescence branches indicate phase transitions and metastable behaviour, with deliquescence occurring at higher RH and efflorescence at lower RH. ....43
- Figure 2.4: This is a satellite image showing a thick blanket of haze and air pollution over northern India and parts of Pakistan. The haze appears to be concentrated over the Indo-Gangetic Plain, including cities like Delhi (NASA Observatory). ....46
- Figure 2.5: Diel variation of Chloride Concentration, Temperature, and Relative Humidity during winter (2021) in Delhi. ....49
- Figure 2.6: Banana curve illustrating new particle formation (NPF) event (13 March 2022), showing the evolution of particle size distributions over time. The plot captures the characteristic growth of nucleation-mode particles, starting from nucleation mode (<25 nm) in the early afternoon (~12:00) and expanding into larger sizes (>50 nm) by midnight. ....52
- Figure 3.1: Geographical representation of the sampling site in South Delhi, India. The top-left panel shows the location of Delhi within northern India, while the top-right panel highlights the administrative divisions of Delhi, marking the sampling site in the southern region. The bottom panel provides a satellite image with the precise sampling location indicated. ....78

Figure 3.2: Schematic of the Instrumentation Setup: The diagram illustrates the aerosol sampling and analysis system, with red-dashed lines indicating a well-maintained and air-conditioned room to ensure stable environmental conditions. Various instruments, including cyclones and analytical devices, are integrated for efficient sample collection and measurement. ....82

Figure 4.1: Temporal trends of chemical composition of PM<sub>2.5</sub> measured in Delhi: organic (Org), nitrate (NO<sub>3</sub>), sulphate (SO<sub>4</sub>), ammonium (NH<sub>4</sub>), and chloride (Cl) concentrations, during (a) 2019-2020, and (b) 2020-2021 winter campaigns. Heavy pollution episodes (HPEs) are shown in shaded grey regions. The dominance of organics is evident, with episodic peaks in PM<sub>2.5</sub> concentrations during HPEs. ....94

Figure 4.2: Average mass contributions of NR-PM<sub>2.5</sub> components (ug/m<sup>3</sup>) at low (<60 %) and high (>60 %) RH conditions. RH = 60% is often considered a critical threshold for aerosol phase transitions, as ambient aerosols undergo physical transformations from a semisolid to a liquid state when RH exceeds this value. The dominance of organics is observed under both RH conditions, with variations in secondary inorganic aerosol contributions. ....95

Figure 4.3: Time series of non-refractory PM<sub>2.5</sub> (NR-PM<sub>2.5</sub>, blue, left y-axis), aerosol liquid water content (ALWC, red, right y-axis), and relative humidity (RH, green dashed line, right y-axis) for two different winters: (a) 2019-2020, and (b) 2020-2021.....98

Figure 4.4: Average contribution of NR-PM<sub>2.5</sub> components (organics, NH<sub>4</sub>Cl, NH<sub>4</sub>NO<sub>3</sub>, (NH<sub>4</sub>)<sub>2</sub>SO<sub>4</sub>) to aerosol liquid water content (ALWC) uptake, categorized by RH bins in 10% increments. The contribution of hygroscopic species such as ammonium nitrate and chloride increase with RH, while the influence of organics varies. The figure highlights the dominant role of inorganic species in ALWC uptake, especially under high-humidity conditions..... 104

Figure 4.5: Relationship between aerosol liquid water content (ALWC) and relative humidity (RH) for different inorganic mass fractions during (a) 2019-2020 and (b) 2020-2021 winters. The plots shows both data points and exponential fits ( $y = \exp(a + bx)$ ). The data points are categorized by inorganic fraction, with black representing the lowest inorganic content (<0.2) and red representing the highest (>0.5). Higher inorganic fractions lead to greater ALWC uptake, particularly at high RH, highlighting the strong hygroscopicity of inorganic aerosol components. .... 107

Figure 4.6: Diel variations of mass concentrations of NR-PM<sub>2.5</sub> inorganic components for (a) 2019-2020, and (b) 2020-2021 winters; Diel variations of NR-PM<sub>2.5</sub> and AWLC mass concentrations for (c) 2019-2020, and (d) 2020-2021 winters; Diel variations of RH and T for (e) 2019-2020, and (f) 2020-2021 winters..... 108

Figure 4.7: Variation of enhanced light scattering coefficient f(RH) with RH; Comparison between visibility-derived and hygroscopicity-derived f(RH). Data is fitted by the exponential function  $y=e^{(a+bx)} +c$ . The fitting parameters for modelled and visibility derived f(RH) vs RH were (a = -10.74, b = 0.123, c = 1.12) and (a = 10.44, b = 0.125, c = 1.14), respectively. The correlation coefficient (R<sup>2</sup>) value for both cases was >0.94. .... 112

Figure 5.1: Seasonal variation in average particle number concentrations of (a) nucleation mode, (b) Aitken mode, (c) accumulation mode, and (d) total, depicted using violin plots. These plots display the distribution and density of concentrations with the central white dot inside each box indicating the median value. The data reveal that total particle number concentration peaks during colder seasons (winter and post-monsoon), while the nucleation mode is more prevalent in warmer periods and the accumulation mode is more pronounced during colder periods..... 135

Figure 5.2: Average diel variation in particle number concentrations for (a) nucleation mode, (b) Aitken mode, (c) accumulation mode, and (d) total for different seasons. .... 138

Figure 5.3: (a) and (b) Typical Type I NPF events. A nucleation mode appears at around 11 AM (LT) and undergoes condensational growth. This can also be observed from the temporal variation of nucleation mode of particles which started to increase at 11 AM. (c) A type II NPF event; no prolonged growth and hence a typical banana could not be observed. (d) A non-NPF event with no feature of NPF identification observed. .... 140

Figure 5.4: (a) Average daily variation of PM<sub>2.5</sub> (µg m<sup>-3</sup>) vs. CS (s<sup>-1</sup>) marked and coloured as the function of RH and (b) average daily variation in the H<sub>2</sub>SO<sub>4</sub> proxy concentration (molecules cm<sup>-3</sup>). Each data point is the average of the variable from 10:00 to 16:00 LT. No NPF event was observed when average daytime CS was above 0.06 (s<sup>-1</sup>), most of which were observed in colder post-monsoon and winter periods. H<sub>2</sub>SO<sub>4</sub> was also lower during these days. The figure highlights that NPF events were absent on some days despite higher H<sub>2</sub>SO<sub>4</sub> and lower CS values. Vertical dashed red lines are included to delineate different CS regions..... 144

Figure 5.5: (a) Average daily variation in the H<sub>2</sub>SO<sub>4</sub> proxy concentration (molecules cm<sup>-3</sup>) versus CS (s<sup>-1</sup>). No NPF event was observed when the average daytime CS was above 0.06 s<sup>-1</sup>, primarily observed during colder post-monsoon and winter periods. While H<sub>2</sub>SO<sub>4</sub> proxy concentrations were comparatively higher on NPF days, the difference does not appear statistically significant. (b) variation of NH<sub>3</sub> vs. CS during NPF and non-NPF days. (c) and (d) Average daytime variation of RH and ALWC (μg m<sup>-3</sup>) versus CS (s<sup>-1</sup>). In lower CS bins (<0.02 s<sup>-1</sup>), high ALWC on non-NPF days led to enhancement in CS of particles and consequently hindering NPF. In the moderate CS bins (0.02 to 0.06 s<sup>-1</sup>), lower RH and lower ALWC favoured NPF. Each data point represents the average of the variable from 10:00 to 16:00 local time (LT). ..... 146

Figure 5.6: Relationship between H<sub>2</sub>SO<sub>4</sub> concentration (cm<sup>-3</sup>) and condensation sink (CS, s<sup>-1</sup>) across various locations. The color of the markers represents the particle formation rate (cm<sup>-3</sup> s<sup>-1</sup>), with higher formation rates indicated by warmer colors. Observations from Delhi are compared with those from other regions, revealing that the new particle formation (NPF) rates in polluted environments are significantly higher than those in relatively clean areas. This trend aligns with global observations, (Cai et., 2023; Deng et al., 2020) highlighting the influence of elevated precursor concentrations and higher CS in polluted regions on NPF processes. .... 148

Figure 5.7: (a) Comparison of chemical composition of PM<sub>2.5</sub> during the daytime for NPF and non-NPF days under different CS bins during the daytime; (b) and (c) difference in the chemical composition of PM<sub>2.5</sub> between NPF and non-NPF days during the days with similar daytime CS and daytime H<sub>2</sub>SO<sub>4</sub> vapour concentrations. All the daytime averages have been estimated during the time interval of 10:00 LT to 16:00 LT for each day..... 153

Figure 5.8: Diel variation of average composition of PM<sub>2.5</sub> during clean and polluted days of the spring season. Sulphate and oxygenated organic aerosols (LVOOA2) dominated the mass fractions of inorganics and organics, respectively, during the daytime when observed NPF events take place in our study during both clean and polluted periods. .... 157

Figure 5.9: Temporal variation of particle size distribution, mode PN concentrations, along with chemical composition of PM<sub>2.5</sub> on two consecutive days, with the first one an NPF. Sulphate and LVOOA2 dominated the mass composition of PM<sub>2.5</sub> between the periods of start of NPF (10:00 LT and 18:00 LT) and end shaded by the light orange colour in plots. This type I growth is interrupted by primary emissions in the evening hours and undergoes night-time rapid growth

due to coagulation between particles and condensation of vapours resulting from low RH and T, represented by the grey shaded regions in the above plots. The primary nature of these processes is validated by the increase in the mass concentration of BC, HOAs and BBOAs along with their enhancement in mass fractions. Semi volatile inorganics such as nitrate and chloride condense at the later stages of the particle growth. .... 159

Figure 6.1: (a, b) A mobile van (CARLab) equipped with real-time air quality monitoring instruments stationed near agricultural fields where crop residue burning is occurring. (c) Schematic of the van equipped with different PM<sub>2.5</sub> characterization (XACT, ACSM, and Aethalometer) and gas analysers (Courtesy: Pandey et al., under preparation). .... 182

Figure 6.2: Seasonal variation of Cl and other PM<sub>2.5</sub> species during the entire sampling period (2019–2022) at the IIT Delhi sampling site, measured using XACT (for K), Aethalometer (for BC), and ACSM (for organics and NH<sub>4</sub>). .... 186

Figure 6.3: The diel variation of Cl and other components during different seasons is observed. Cl diel plot is characterized by an early morning sharp peak, which is more pronounced than for other species. .... 188

Figure 6.4: Combined PMF of elemental PM<sub>2.5</sub> and BC identified biomass burning and secondary chloride factor profiles during the post-monsoon period in Delhi, 2022. .... 189

Figure 6.5: (a) Temporal variation of PM<sub>2.5</sub> species during the sampling period in Punjab. (b) Average chemical composition over the sampling period, excluding the Diwali period. .... 190

Figure 6.6: Diel variation of key biomass burning tracers Cl, K, BC and Organics during Punjab sampling. .... 192

Figure 6.7: (a) Stubble burning factor profile obtained from PMF analysis during Punjab sampling period of stubble burning; (b) Relative contribution of different factors to total elemental PM<sub>2.5</sub> and BC concentration. .... 193

Figure 6.8: (a) Temporal variation of mass concentration of organics and stubble burning factor profile obtained from PMF analysis during Punjab sampling period of stubble burning; (b) Comparison of diel variations of stubble burning factor and aethalometer model apportioned biomass burning BC (BC<sub>bb</sub>) factors to total elemental PM<sub>2.5</sub> and BC concentration; (c and d)

Scatter plots of stubble burning factor vs BC and K; and (e) Diel plots of stubble burning factor and Cl. .... 194

Figure 6.9: (a) Stubble burning factor profile obtained from PMF analysis during Punjab sampling period of stubble burning; (b) Relative contribution of different factors to total elemental PM<sub>2.5</sub> and BC concentration. .... 197

Figure 6.10: Time series of chemical components in PM<sub>2.5</sub> measured during winter and spring in Delhi. Two types of periods have been identified: the high-chloride and high-organics episode (shaded by blue colour) and the high-chloride and low-organics periods (shaded by magenta colour). .... 199

Figure 6.11: Scatter plot of Cl:BC versus Cl:OC ratios for various type of burning as collected from literature, compared with measured ratios from the present observations from Delhi and Punjab. .... 200

## List of Tables

Table 4-1: : Average mass concentrations ( $\mu\text{g}/\text{m}^3$ ) of NR-PM<sub>2.5</sub>, ALWC, Inorganics, Organics, SO<sub>4</sub><sup>2-</sup>, NO<sub>3</sub><sup>-</sup>, NH<sub>4</sub><sup>+</sup>, Cl<sup>-</sup>, and meteorological parameters (RH, T, and wind speed) under different pollution conditions during 2019-2020 and 2020-2021 winter seasons. ....99

Table 6-1: Seasonal variation of average chloride concentrations (in  $\mu\text{gm}^{-3}$ ) in Delhi from different studies. The values for Nov 2019–Dec 2022 represent the present study, while previous studies provide comparative data. ....186